Desalination and Water Treatment
www.deswater.com
doi: 10.5004/dwt.2022.28051

249 (2022) 297–308
February

Photocatalytic treatment of spontaneous petrochemical effluents by TiO_2 CTAB synthetic nanoparticles

Amin Ahmadpour[a], Alireza Bozorgian[b,*], Ali Eslamimanesh[c], Amir H. Mohammadi[d]

[a]*National Petrochemical Company, Petrochemical Research and Technology Company – Mahshahr Centre, Mahshahr, Iran, email: Aminahmadpour18@gmail.com*
[b]*Department of Chemical Engineering, Mahshahr Branch, Islamic Azad University, Mahshahr, Iran, email: a.bozorgian@mhriau.ac.ir*
[c]*Department of Process Engineering, Faculty of Chemical Engineering, Tarbiat Modares University, Tehran, Iran, email: ali.eslamimanesh@modares.ac.ir*
[d]*Discipline of Chemical Engineering, School of Engineering, University of KwaZulu-Natal, Howard College Campus, King George V Avenue, Durban 4041, South Africa, email: amir_h_mohammadi@yahoo.com*

Received 12 June 2021; Accepted 2 January 2022

ABSTRACT

Removal of pollutants from petrochemical effluents is vital in terms of effluent control and achieving environmental standards. Because of the nature of particular effluents in petrochemical industry, direct biological treatment is not recommended. Therefore, novel techniques such as advanced oxidation processes through photocatalytic processes have been proposed for this purpose. In this study, synthetic photocatalyst TiO_2-CTAB (cetyletrimethylammonium bromide) was used for treatment of a real spent-neutral effluent from a neutralization section of the olefin unit of a petrochemical plant. In order to study the chemical oxygen demand (COD) of the process, a double-walled photoreactor was utilized pursuing the Box–Behnken experiment design method. The results show that increasing the concentration of photocatalyst at neutral pH, up to an optimal value of 0.61 g/L in unrestricted conditions and 2 g/L in restricted conditions enhances COD removal by 91.3% and 90.7%, respectively. Furthermore, the effects of oxidation parameters, aeration rate, pH and the amount of catalyst loaded on COD removal efficiency were investigated. It is interpreted from the results that when the oxidant is at its lowest level, removal efficiency is reduced with increasing pH.

Keywords: Photocatalytic effluent treatment; Spontaneous caustic; Titanium dioxide; Experimental design; Chemical oxygen demand; CTAB nanoparticles

1. Introduction

Industrial wastewater streams are major sources of toxic inorganic/organic compounds to the environment particularly to natural waters. The amounts of these streams are substantial and can be up to 10^{10} t/y in, for instance, the mainland China. In an industry vertical such as petrochemical downstream operation, the hazardous effluent discharged to the surroundings is not only obvious but also of significant concern. The issue is more pronounced knowing that biological methods for treating these kinds of wastewaters are often not feasible due to the resistance of their contaminants to biodegradation [1–4].

Currently, there are various types of petrochemical wastewater treatment methods depending on the properties of the effluent including concentrations of the contaminants and operational parameters such as the chemical oxygen demand (COD) [5]. An industrially-viable treatment technique for a petrochemical facility typically contains

* Corresponding author.

mechanical pre-treatment processes as well as further removal operations using activated sludge etc. [1–5] However, high concentrations of the pollutants in the effluents accompanied by relatively large values of COD parameter are the bottlenecks of this conventional process [3–5]. Therefore, efforts have been focused on developing more viable methods for such treatments.

The effluent treatment process through advanced oxidation processes (AOP) is based on the production of highly active species such as hydroxyl radicals which are able to rapidly oxidize a wide range of organic pollutants. Moreover, the AOPs are feasible in wide ranges of operational temperature and pressure conditions which have made them very attractive from practical point of view. Although AOPs are generally suitable for treating wastewaters with COD values up to 5,000 mg O_2/L, vast majority of the petrochemical effluents suffer from having higher orders of magnitudes of COD [1,6]. For this reason, improving the advanced oxidation processes is an imperative area of research.

Heterogeneous photocatalysis is a type of advanced oxidation processes utilizing a photocatalyst in the heterogeneous phase in the presence of ultraviolet (UV) light [7]. This method leads to satisfactory degradation of resistant and toxic organic matters accompanied by negligible amounts of hazardous by-products. Although use of heterogeneous photocatalysts is very common in different forms, low quantum efficiency relative to visible light, photoreactor design, catalyst recovery and reuse, production of toxic intermediates and catalyst inactivation problems are some of the disadvantages of this method. Selection of the type of the catalyst is the major step in designing such processes. In the case that the catalyst is used in the form of suspended particles in the aqueous phase, nanoparticles such as TiO_2 generally show more promising results [8] however other amorphous materials such as ZnO, Fe_2O_3, and WO_3 have been recommended for the same purpose as well [1,6]. Titanium dioxide is a widely used photocatalyst to remove large numbers of organic compounds due to its high photocatalytic activity, non-toxicity, chemical stability and cost-effectiveness [1,6,7].

Considering the costs of ultraviolet light and its possible health risks, developing novel catalysts which can be operated in visible light or even sunlight like photocatalysts are of importance particularly for large scale wastewater treatment plants. Apart from that, accurate knowledge of effect of various factors on the efficiency of the photocatalytic process is required in order to design an effective treatment technique.

In olefin units of petrochemical industry, the exhaust gases from furnaces contain sulfur compounds which are separated from olefins, hydrogen and methane using caustic solution in separation towers. In this process, following the removal of hydrogen sulfide, a toxic and harmful combination of sodium sulfide is observed in the effluent of the unit. The output caustic solution contains sulfur-bearing species and hydrocarbons and has high acidity. Apart from that, its high sulfide content causes toxicity to microorganisms in bio-effluent treatment [9]. Furthermore, sulfide contamination not only can cause severe corrosion damage to the process facilities but also produces sulfur deposits in transportation as well as operational units. The aforementioned characteristics pave the way to develop suitable strategies for treatment of this hazardous waste stream.

Due to the fact that spontaneous caustic effluent contains a wide range of hydrocarbons, the photocatalytic oxidation method for the initial degradation of contaminants prior to biological treatment and following physical pre-treatment seems feasible in large industrial scale. Oxidizing agents such as oxygen or hydrogen peroxide can potentially oxidize sulfide, sulfide-bearing compounds as well as hydrocarbon compounds to the standard levels. However, spontaneous effluents of olefin units contain considerable amounts of salts for which treatments using conventional oxidation methods might lead to environmental concerns. On the other hand, high cost of using UV lamps in the use of the photocatalytic method limits the possibility of optimal use of such methods. Photocatalytic degradation of the aforementioned contaminants depends on the type, composition and amounts of the utilized catalysts, light intensity, raw material concentration, pH of the reaction solution, catalyst application method and calcination temperature. Accurate knowledge of the effect of these factors on the efficiency of photocatalytic treatment process is required in designing optimum and proper treatment plants [2].

A detailed literature review reveals that considerable amount of works have been found in open literature which have investigated the treatment of spontaneous caustic effluent using advanced oxidation techniques. In 2000, Carlos and Maugans [10] studied the treatment of caustic effluent using the wet air oxidation method. They applied 0.2 m^3 of caustic effluent and diluted it with 0.4 m^3 of water at a temperature of 260°C and a pressure of 90 bar. As a result, they succeeded to reduce the COD from 72,000 to 15,000 mg/L.

A combined neutralization-escape-Fenton process has been applied by Sheu and Weng [11] in order to remove more than 94% of COD from the wastewater. The neutralization-evaporation combination was capable of reducing COD accompanied by reducing sulfide from 19,000 to 1,400 mg/L. Moreover, adding the Fenton process to the above sequence operations further reduced COD to about 150 mg/L COD. In 2008, Rodriguez et al. [12] studied the treatment of caustic effluent using the electro-Fenton process. They were able to reduce 95% COD at pH = 4 and 40ºC and at 100 mg/L iron. In a similar effort, 93% of COD was reduced by Nunes et al. [13] to treat caustic effluent using an electrochemical oxidation process.

Yu et al. [14] investigated removal of 68% of COD in a combined UV/H_2O_2/O_3 process for the treatment of caustic effluent. Their outcome shows that UV/H_2O_2 process had 44% efficiency in the COD removal operation. In another work, treatment of caustic effluent through various types of techniques was analyzed by Hawari et al. [15]. They reported 99% sulfide removal at pH = 0.5 and 98% removal of COD. In addition, oxidation by H_2O_2 led to remove 89% of COD at a pH = 2.5 by consuming 19 mM of oxygenated water [15].

The application of photo-Fenton oxidation process for treatment of spontaneous spent effluent was carried out by Sayid Abdulah et al. [16]. Under optimal conditions, they reported a 92% COD removal and a 98% sulfide reduction

from the studied waste stream. In 2013, Chen [17] investigated the treatment of real spontaneous effluent with a COD of 25,000 by conventional and catalytic humidification methods which resulted in 75% and 95% reduction in COD for the conventional method and the catalytic method, respectively. In another attempt, Alaizadeh [18] was able to reduce the COD from a spent effluent of South Pars gas refinery using an electrical coagulation operation. The subsequent results show that the highest efficiency of the process was 91% and its optimal operating conditions were the effective time of 105 min, dilution with a ratio of 2 volumes of effluent and 1 volume of water, acidity equal to 9, current density of 62.8 mA/cm^2 and 1.32 g/L of materials [18].

Typically, surface activators which increase stability and rate of adsorption in aqueous separation systems is added to improve the performances of advanced chemical oxidation treatment processes [19–21]. Such operations are common throughout various industry verticals such as food and pharmaceutical industries which use nanostructured materials. In these systems, the stability of the adsorption operation is controlled by electrostatic, dipole, and hydrophobic forces. In the case that a cationic surface activator is added to the aqueous solution containing the anionic polymer, strong systemic electrostatic interactions will build up in the environment. In fact, surface activators prevent the particles from joining and clumping during synthesis in aqueous environments due to having both hydrophilic and hydrophobic heads. This phenomenon improves the properties of the resulting nanoparticles and reduces the size of the crystal. Furthermore, use of surfactants improves the morphology of nanoparticles and increases porosity to some extent. Among the surfactants recommended to be used in the synthesis of nano-catalysts for wastewater treatment applications, CTAB (cetyletrimethylammonium bromide), TTAB (tetradecyltrimethylammonium bromide), DTAB (Dodecyltrimethylammonium bromide) and ethylene glycol are more common. There are evidences in the literature that show CTAB has the best performance in stable synthesis of nanocrystals [19–21].

The goal of this work was to present an efficient treatment process to be used in removal of contaminants from a real spent-neutral effluent from a neutralization section of the olefin unit of a petrochemical plant. The chemical method here is based on the advanced chemical oxidation utilizing a synthetic photocatalyst TiO_2 CTAB. In order to demonstrate the performance of the treatment unit, the effects of important factors on the performance of the process were studied experimentally.

2. Experiments

2.1. Materials

The waste water stream sample (pH = 7.3) was taken from a real spent-neutral effluent neutralization section of the olefin unit of a petrochemical plant which is then sent to a photo-reactor. The specifications of this effluent are given in Table 1.

Chemicals used in this study and their formula are listed in Table 2. All the chemicals except deionized water were supplied by Merck.

2.2. Photocatalyst synthesis

The photocatalyst was synthesized in the following steps:

- 1.2 g of CTAB was dissolved in water using the sol–gel method and the solution was stirred for 30 min until a gel-like uniform solution was obtained.
- 6 g of $(NH_4)_2SO_4$ was added to the solution and was stirred.
- Then an ice bath was prepared and 2.5 mL of $TiCl_4$ was gradually added to the solution under intense stirring for 1 h.
- The temperature of the solution was raised to 70°C using an oil bath and then the container was placed on a stereo machine and was titrated with 25% NH_4OH until the pH reached 8 and all Ti ions precipitated.
- The formed precipitate was mixed with deionized water and was filtered to separate the Cl^- ions from the

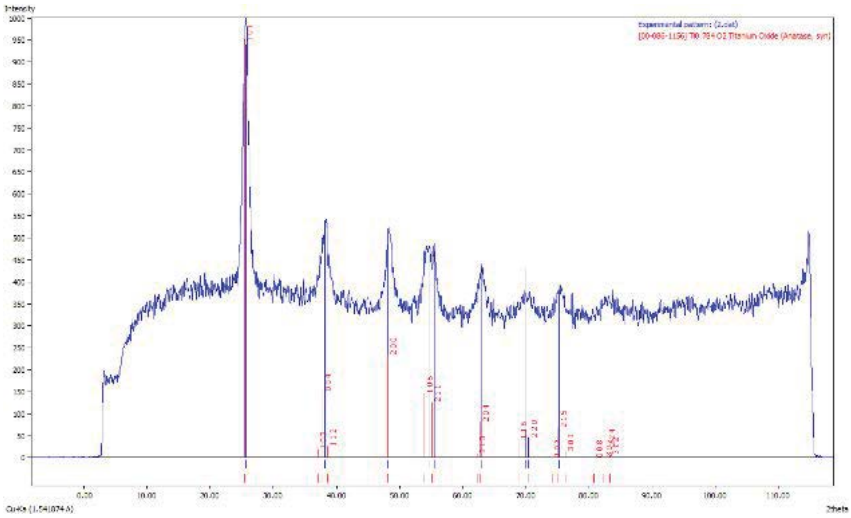

Fig. 1. XRD analysis diagram of TiO_2-CTAB nano-photocatalyst.

Table 1
Specifications of effluent used as feed

Parameter	Amount (ppm)
COD	1,280
BOD	615
Phenol	4.7
TDS	89,000
Sulfide	7.8

Table 2
Chemicals used in this study

Chemical	Chemical formula
Hydrogen peroxide	H_2O_2
Sulfuric acid	H_2SO_4
Caustic soda	NaOH
Potassium dichromate	$K_2Cr_2O_7$
Mercury sulfate	$HgSO_4$
Silver sulfate	Ag_2SO_4
Potassium hydrogen phthalate	$C_8H_5KO_4$
Hydrochloric acid	HCl
Copper sulfate	$CuSO_4$
Sodium sulfide	Na_2SO_4
Cetyltrimethylammonium bromide	$C_{19}H_{42}BrN$
Ammonium sulfate	$(NH_4)_2SO_4$
Titanium tetrachloride	$TiCl_4$
Deionized water	H_2O
Ammonium hydroxide	NH_4OH
Nitric acid	HNO_3

sample. The latter step was taken because the presence of these ions as impurities has negative effects on the optimum catalyst morphology.
- The sample was then placed on a strainer to dry for 12 h at 50°C in a vacuum oven.
- The next step was the peptizing procedure in which the dried sample was weighed and mixed with water to make a uniform solution under rapid agitation. The final pH was brought to 1.5 using 0.65 wt.% HNO_3 solution. The obtained mixture was refluxed for 2 h in an oil bath at 80°C and was kept in a dry and dark cabinet for several days to obtain stable tuber. It was then dried at 60°C in a vacuum oven.
- Finally, the obtained compound was calcined [20] in a furnace with a heating intensity interval of 2°C/min to reach the desired temperature of 400°C at which it was remained for 2 h [22].

2.3. XRD analysis

The XRD pattern of titanium dioxide material has three index peaks in the range 2θ, which are: 25.2 for the level of 101 anatase phase, 27.4 for the level of 110 rutile phase and 30.8 for the level of 210 brookite phase. Fig. 1 shows the XRD pattern of the TiO_2 nano-photocatalyst CTAB. As can be seen, the XRD peaks overlap well with the peaks of the TiO_2 anatase phase. The size of crystals (in angstrom) of the respective phases in the analyzed photocatalyst can be obtained using Scherrer equation as follows:

$$d_c = \frac{B\lambda}{\beta\cos\theta} \tag{1}$$

where B is a constant number between 0.9 and 1.00, λ is the wavelength of the device source (in angstrom), β is the width at half the maximum peak or FWHM (in radians), and θ is the Bragg angle. Moreover, the weight fraction of the anatase phase in the mixture can be determined using the Spore/Myers ratio as follows:

$$W_A = \frac{1}{\left(1+\frac{1.26I_R}{I_A}\right)} \tag{2}$$

where W_A is the weight fraction of the anatase phase in the mixture and I_A and I_R are the peak diffraction intensities of anatase and rutile phases, respectively. Consequently, crystal observed of anatase phase is estimated to be 25.4 nm and the weight percentages of crystal phases are estimated to be 78% for the anatase phase and 22% for the rutile phase.

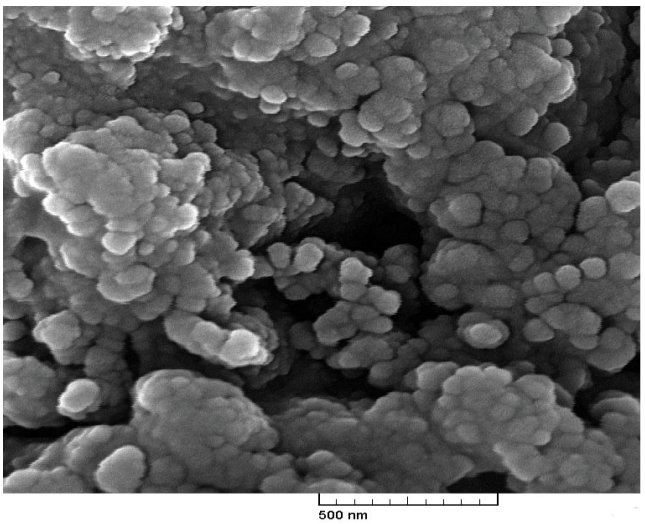

Fig. 2. SEM image of nano-photocatalyst TiO_2-CTAB.

The SEM analysis of the nano-photocatalyst TiO_2-CTAB is observed in Fig. 2 which indicates that the corresponding calculations provide a mean size of 29.8 nm for the particle. The DRS (diffuse reflectance spectroscopy) experiments, shown in Fig. 3, were undertaken on the photocatalyst in order to observe the amount of light scattering and absorption in the wavelength range of 800–300 nm for calculating the energy gap.

2.4. Determination of the zero-load point

The zero-load point or point of zero charge (pzc) of the produced photocatalyst defines the pH where the

density of the electric charge on the surface of the catalyst is zero. For TiO_2, this pH is generally in the range of 5.6–6.4. At a pH lower than pzc, the molecule level will have a positive charge due to the presence of H^+ ions meanwhile at a pH higher than pzc, the electric charge on the TiO_2 surface is negative due to the presence of negative OH^- ions. Regarding the applied photocatalyst herein, this means that at pH > zpc, the catalyst particles present in the aqueous solution are mostly TiO^- and at pH < zpc, $TiOH^{+2}$ particles with a positive charge are predominant [14]. Another reason for the importance of pH during the photocatalytic process is the acidity of the contaminant. The hydroxyl groups on the TiO_2 surface under acid and base conditions pursue the following equilibria:

$$TiOH_2^+ \xrightarrow{pK_{a1}^s} TiOH + H^+ \quad (3)$$

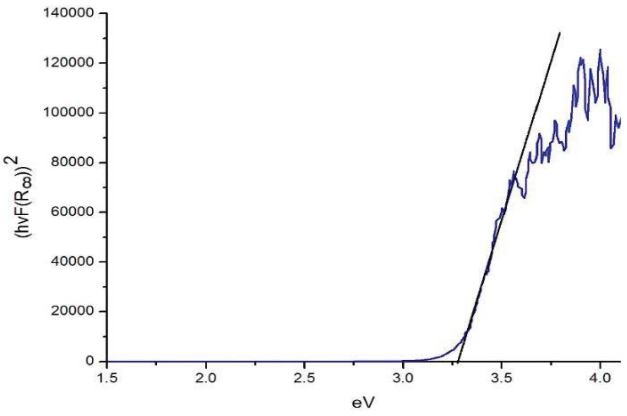

Fig. 3. Graph of hvF (($R\infty$)^2) in terms of electron volts for the TiO_2-CTAB nano-photocatalyst.

$$TiOH \xrightarrow{pK_{a2}^s} TiO^- + H^+ \quad (4)$$

In the above reactions, pK_a^s denotes the surface acidity which is assumed to be constant. Accordingly,

$$pH_{zpc} = \frac{1}{2}\left[pK_{a1}^s + pK_{a2}^s\right] \quad (5)$$

As seen in Fig. 4, the zpc value of the photocatalyst used in this study was determined to be 6.6 following the relevant experimental data analysis procedure [23].

2.5. Photoreactor specifications

The schematic of the photoreactor used in this study is shown in Fig. 5. All oxidation reactions were performed in this mixed double-walled photoreactor which has been made of 304 stainless steel operated under atmospheric conditions. The photocatalyst was used sparsely

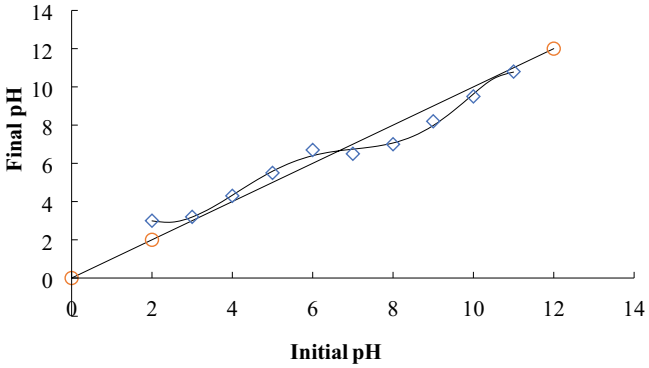

Fig. 4. Diagram of zpc of nano-photocatalyst TiO_2-CTAB.

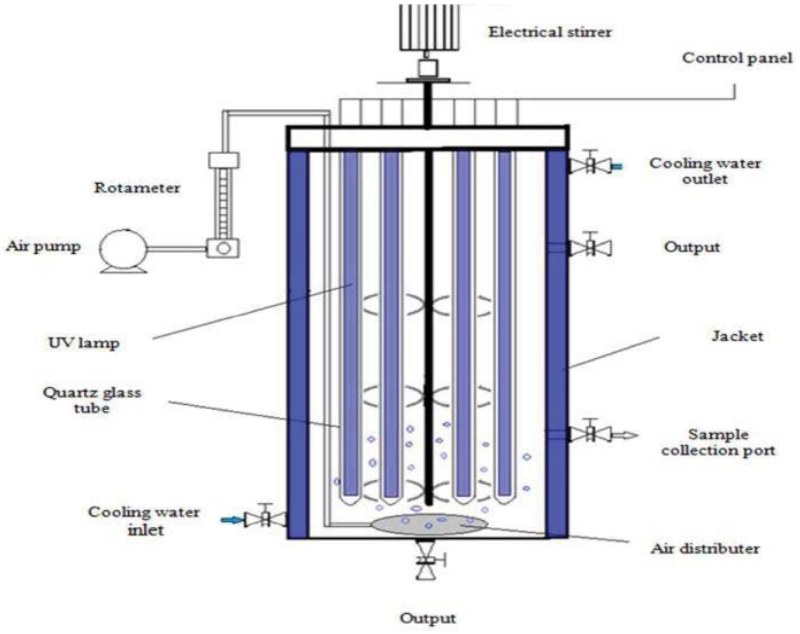

Fig. 5. Schematic diagram of the photoreactor.

in solution (in the form of slurry). In the applied reactor, eight 16-watt UV lamps were made by eight quartz glasspods. In order to place the lamps inside the photoreactor, tubes with a size of 2.45 cm of quartz were used vertically in the desired locations. The distance between the lamps should be the same to make the intensity of light uniform throughout the reactor. During the experiment, an aluminum foil was used on the reactor inlet to prevent light from emitting into the environment. Furthermore, for blocking the space around the quartz glass after installation in the reactor, a Wheaton washer was applied.

The solution inside the reactor was mixed using a vane stirrer with three blades which was adjusted by a 12-V DC electric motor at 200 rpm. The aeration required for the solution was provided by a Heila compressor with a capacity of 35 min^{-1}. A circular aquarium sparger was injected to create smaller bubbles and to properly distribute the air in the system. The photo-reactor was equipped with a cooling water jacket to control the temperature.

2.6. Main test procedure

In the beginning of the experiments, a sample from the content of the photoreactor and its COD value was taken. During the photocatalytic reaction test (90 min), a 2 mL sample from the contents of the reactor was collected and measured for the corresponding COD value. For this purpose, the method Laboratory No. 5220 of APHA standard was used. Moreover, the APHA standard No. D-5530 and methylene blue methods were pursued in order to measure the amounts of phenol and dissolved sulfides in the sample effluent, respectively [23].

In this study, the photocatalytic removal efficiency of COD at 90 min was selected as the response (objective function) which can be calculated using Eq. (6):

$$\text{Degradation efficiency}\,(\%) = \frac{C_0 - C}{C_0} \times 100 \tag{6}$$

In this equation, C_0 and C are, respectively, the COD values at the beginning of the photocatalytic process (bright moment lamps) and at 90 min when the sample was taken from the products [24].

2.7. Analyzed factors

Four factors of photocatalyst concentration (*A*), acidity (*B*), auxiliary oxidation concentration (hydrogen peroxide) (*C*), and aeration rate (*D*) were analyzed during the experiments as the main factors affecting the photocalytic process. Table 3 summarizes the levels of the aforementioned factors during the experiments.

In order to develop a correlation between the response and independent variables (selected experimental factors), the Box–Behnken (RSM) surface response experiments (RSM) design method was employed. The form of the correlation is shown in Eq. (7):

$$y = \beta_0 + \sum_{i=1}^{k} \beta_i x_i + \sum_{i=1}^{k} \beta_{ii} x_i^2 + \sum_{1 \le i \le j}^{k} \beta_{ij} x_i x_j + \varepsilon \tag{7}$$

where y is the response variable or the percentage of COD depletion, β_0 is constant, β_{ij}, β_{ii}, β are interaction coefficients, x_j x_i are independent variables and ε is a random error rate.

In this work, 30 experiments were undertaken with six duplicate points. Accordingly, optimal COD removal conditions were determined for the system of interest.

3. Results and discussion

3.1. Screening test design

For screening studies, the use of two levels for each factor can generally be well responsive. In the present method, two levels (1– and +1) are selected for each factor. Then, the minimum number of orthogonal experiments is determined and the experiments are done on this basis. Eventually, through use of the experimental outputs, a linear model in the form of $z = b_0 + \sum b_i \cdot x_i$ is developed where z is the response, b_0 is the width of the origin, b_i is the linear coefficient, and x_i is the level of the independent factors. In this work, the results of statistical studies reported on the degradation of other pollutants were studied in the first place. Subsequently, factors and appropriate levels with a wide range of changes were considered to perform a comprehensive analysis.

3.1.1. Selected factors

Following the aforementioned procedure, the selected effective factors on the COD removal efficiency were selected for analysis:

- Temperature (°C)
- Aeration rate (min^{-1})
- Light intensity in terms of number of lamps lit
- Auxiliary oxidizing concentration of hydrogen peroxide in (ppm)

Table 3
Amplitude and levels of selected factors

Factor	Sign	Level code of each variable	
		Below (1–)	Top (1+)
Photocatalyst concentration (g/L)	*A*	0.5	2
pH	*B*	4	10
Oxidizing concentration (ppm)	*C*	0	300
Aeration rate (min^{-1})	*D*	0.5	4

- pH
- Catalyst loading, (g/L)

As already described, a 2 Level Factorial method was used in designing the screening test here which resulted in 16 experiments according to the selected operational conditions. Furthermore, the photocatalytic removal efficiency of COD in 90 min was selected as the objective function.

3.2. Results of screening test

The screening experiments showed the following order of effectiveness of each investigated factor on the removal efficiency:

- Light intensity
- Concentration of loaded photocatalyst
- Auxiliary oxidizing agent (H_2O_2) concentration
- Initial pH
- Aeration intensity
- Temperature

In order to optimize the process and evaluate the factors, the exposure factor was set to its maximum value (8 incandescent lamps) and the temperature factor was removed from the analysis due to minor changes during the reaction. The results of the main experiments are tabulated in Table 4.

3.3. Numerical analysis

On the basis of the obtained experimental results, the following model was obtained:

$$R = -38.09 + 10.57254 \times \mathrm{pH} + 0.157 \times C_{H_2O_2} + 32.7 \times \mathrm{Air} + 3.97 \times \mathrm{Catalyst\ Loading} \times \mathrm{pH} - 0.11916 \times \mathrm{Catalyst\ Loading} \times C_{H_2O_2} - 6.05 \times (\mathrm{Catalyst\ Loading}) \times \mathrm{Air} + 0.032 \times \mathrm{pH} \times CH_2O_2 - 0.025 \times C_{H_2O_2} \times \mathrm{Air} - 6.47 \times \mathrm{Catalyst\ Loading}^2 - 1.65 \times \mathrm{pH}^2 - 2.70641\mathrm{E}\text{-}004 \times C_{H_2O_2^2} - 3.38 \times \mathrm{Air}^2 \quad (8)$$

Table 4
Main experimental data obtained

Set	Catalyst load (g/L)	pH	Oxidizing agent (ppm)	Aeration rate (min^{-1})	Experimental COD value (%)	Quantity COD test design value (%)
1	1.25	7	150	2.25	85.3	84.8
2	1.25	7	300	0.5	78.2	78.9
3	2	10	150	2.25	75.6	78.1
4	1.25	7	150	2.25	83.2	84.1
5	2	7	300	2.25	89	87.3
6	0.5	10	150	2.25	40.2	37.3
7	1.25	10	0	2.25	28.1	27.7
8	5	7	150	0.5	38.8	403
9	1.25	7	300	4	85.1	86.5
10	0.5	7	0	2.25	32.4	35.3
11	1.25	4	150	0.5	55.2	56
12	2	7	150	0.5	81.8	79.7
13	1.25	7	0	0.5	36	36
14	1.25	7	0	4	70.5	71.2
15	1.25	7	150	2.25	87.2	87.1
16	1.25	7	150	2.25	83.3	83.9
17	2	7	0	2.25	85.1	85.5
18	0.5	7	150	4	76.3	76.7
19	1.25	10	300	2.25	83.2	83
20	1.25	4	0	2.25	73.2	71.9
21	0.5	4	150	2.25	73.8	71.4
22	1.25	4	300	2.25	70.5	71.7
23	1.25	10	150	0.5	39.1	40
24	0.5	7	300	2.25	89.4	90.2
25	1.25	10	150	4	60.3	61.7
26	1.25	4	150	4	79.2	78.7
27	2	7	150	4	87.3	85.4
28	1.25	7	150	2.25	82.7	84.4
29	2	4	150	2.25	73	77.3
30	1.25	7	150	2.25	84.6	84.3

in which R denotes the response or the COD removal efficiency, $C_{H_2O_2}$ stands for the concentration of oxidizing agent (ppm), air is the aeration rate (min^{-1}), catalyst loading is the concentration of loaded photocatalyst (g/L), and pH is the initial pH value. For further analysis of the obtained model, statistical tests such as analysis of variance were used.

Table 5 shows the results of variance analysis and the other statistical parameters of the obtained quadratic polynomial model [Eq. (8)]. As can be seen, the model is statistically valid. According to the numerical analysis, the term BD (which stands for interaction of aeration rate and pH) was removed from the model final equation due to its insignificance.

3.4. Diagnostic plots

Fig. 6 shows the parity plot of predicted values of COD removal efficiency from the aforementioned model against the experimental data. In general, a good agreement between the predicted values and the experimental data was observed. Furthermore, the effects of the studied parameters on the rate of COD removal are plotted in Fig. 7 in the form of three-dimensional response surface diagrams and corresponding contour line diagrams. These contour plots show the effects of amount of catalyst loading and pH at fixed amount of aeration rate and 3 levels of oxidant on the efficiency of COD removal from the effluent.

Table 5
Analysis of variance and other statistical parameters of the model

Model parameter terms	Sum of squares	Mean square	F-value	p-value probability > F
	10,970.84	816.15	159.45	<0.0001
A: Catalyst loading (g/L)	1,713.12	1,627.56	285.67	<0.0001
B: pH	829.41	815.89	135.56	<0.0001
C: $C_{H_2O_2}$ (ppm)	2,589.12	2,459.67	465.89	<0.0001
D: Aeration rate (min^{-1})	1,423.43	1,379.12	278.08	<0.0001
AB	335.12	313.19	55.12	<0.0001
AC	756.12	717.65	138.17	<0.0001
AD	277.48	258.23	41.56	<0.0001
BC	834.27	830.12	149.19	<0.0001
CD	167.95	172.19	31.9	<0.0001
A^2	95.19	97.18	15.67	0.001
B^2	1,601.21	1,502.45	289.3	<0.0001
C^2	257.25	284.17	44.28	<0.0001
D^2	785.12	743.56	131.16	<0.0001
Residual	88.19	5.97	–	–
Lack of fit	70.14	6.14	1.71	0.2613
Pure error	18.05	3.6	–	–

Adequate precision = 38.623, PRESS = 411.25, R^2 = 0.9903, Adjusted R^2 = 0.9836, Predicted R^2 = 0.9646, RMSE = 0.358, MAE = 0.318, Absolute average deviation (AAD) = 0.88.

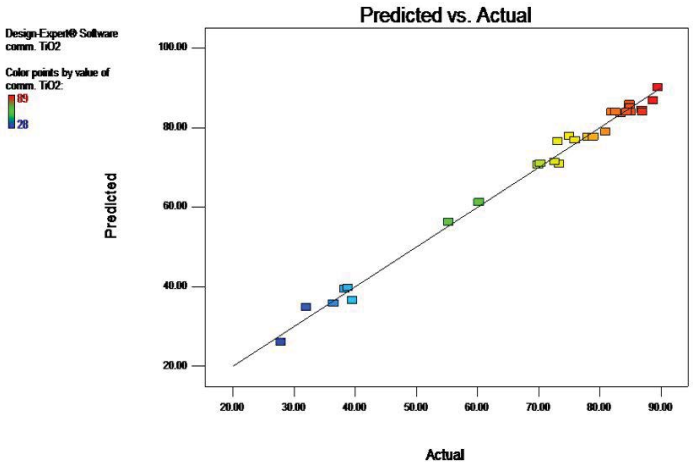

Fig. 6. Parity plot between the predicted and experimental COD removal efficiency.

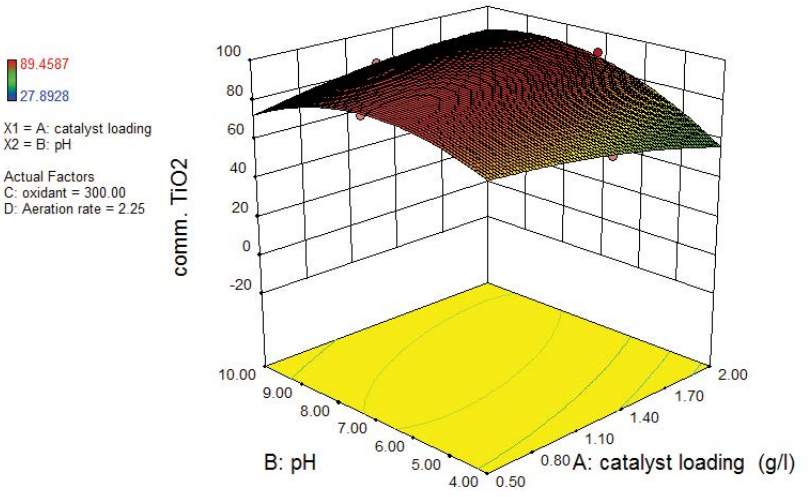

(a)

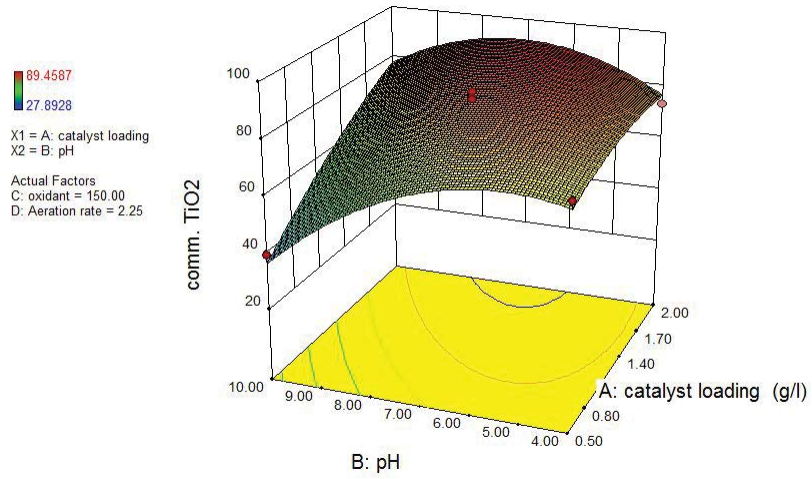

(b)

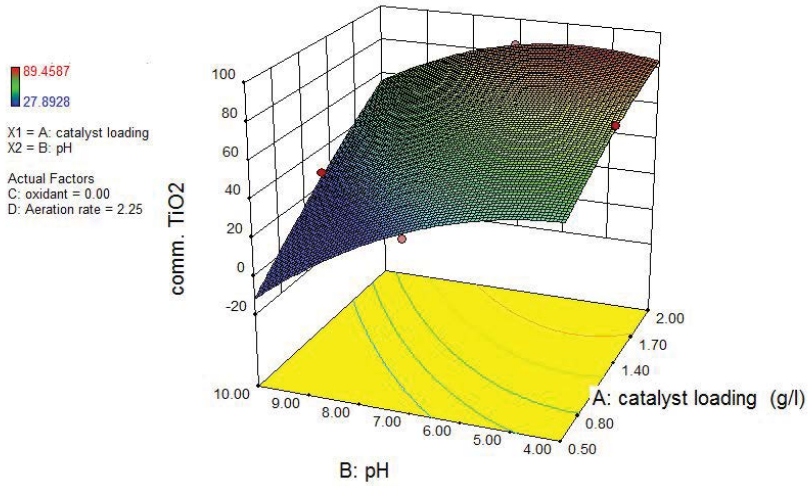

(c)

Fig. 7. Three-dimensional representations of changes in the COD removal efficiency as a function of investigated factors at (a) maximum amount of auxiliary oxidizer, (b) average amount of auxiliary oxidizer and (c) minimum amount of auxiliary oxidizer.

It is well established that higher pH values are needed to prevent agglomeration at higher concentrations of photocatalysts. The obtained experimental data herein reveal that when the photocatalyst concentration is at its lowest level, by increasing the pH from 4 (weakly acidic) to 10 (weakly basic), the COD removal efficiency decreases. In the case of photocatalyst concentration increase, the rate of change of COD removal declines due to the pH augmentation and will finally reach a constant value (a plateau). On the other hand, when the pH is at its lowest level, the rate of COD removal increases linearly with increasing oxidizing agent concentration and as the pH increases, there is an enhancement in the slope of COD removal changes as well. It is also observed from the measured data that when the oxidant concentration is in its middle range, it has the most significant impact on other investigated factors and increases the COD removal efficiency quite considerably. Moreover, the plots indicate that for lower levels of the photocatalyst, acidic pH conditions are more suitable to reach a high level of COD removal efficiency.

4. Optimization of the investigated factors

In order to reach the optimum values of the investigated factors, the following methods were pursued:

- Limitless optimization in which no attempt was made to adjust the number of factors.
- Constrained optimization in which the number of effective factors was adjusted.

In non-factor optimization, all factors were kept in their respective ranges and the removal rate of COD, which was considered as a function of the target (decision) variables was maximized as shown in Table 6. Table 7 summarizes the values of the optimal variables and the subsequent optimized COD removal percentage. A can be seen from the results, the maximum COD removal percentage using the presented treatment process is estimated to be 91.3%.

In order to compare the obtained results with the other contaminant removal techniques, the COD removal efficiency data collected from the adsorption, photolysis and photocatalytic adapters have been plotted in Fig. 8. As expected, adsorption and photolysis adapters have shown to present very little effect on COD removal efficiency

Table 7
Percentage of COD removal at the obtained optimal conditions

Method of optimization	Limitless	Constrained
COD removal, %	91.3	90.7
Aeration rate (min^{-1})	2.5	3
$C_{H_2O_2}$, ppm	290	0
pH	6.55	7
Catalyst loading (g/L)	0.61	2

Table 6
Obtaining optimal values of the effective factors in COD removal process

Factor	Upper limit	Lower limit	Method of optimization	
			Limitless	Constrained
			Target values	
A: Catalyst loading (g/L)	2	0.5	In range	In range
B: pH	10	4	In range	Target = 7
C: C_{H2O2}, ppm	300	0	In range	Minimize
D: Aeration rate (min^{-1})	4	0.5	In range	In range
COD removal, %	89.4	28.1	Maximize	Maximize

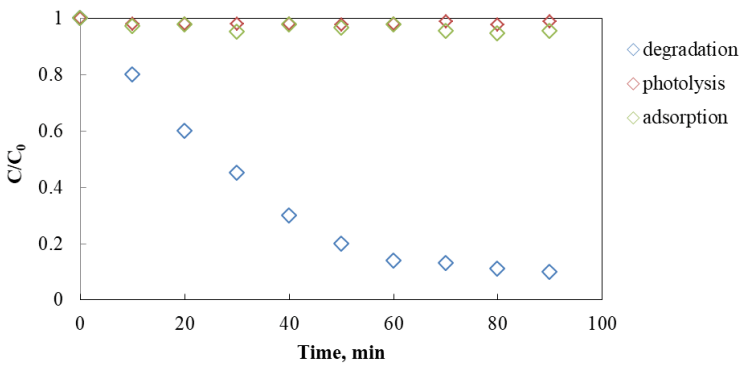

Fig. 8. Comparison between adsorption, photolysis and photocatalyst adapters for COD removal process as a function of operation time.

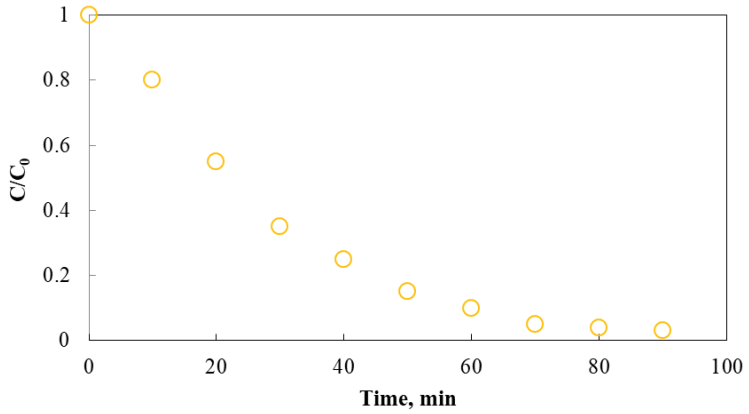

Fig. 9. Graph of phenol removal in sample effluent as a function of operation time.

compared to the photocatalyst process. Another example of the efficiency of the presented removal method can be demonstrated in Fig. 9 which shows the removal of phenol in the sample effluent during the experiment by photocatalytic process under optimal conditions which is around 97%. In Fig. 9, C and C_0 stand for the fraction of phenol removal during and at the end of the removal process.

Finally, the percentage of sulfide removal in the sample effluent for 90 min of operation and at the average values of the investigated factors was obtained to be 4.19%, which shows that the photocatalytic process has little effect on the sulfide removal for the system of interest. Indeed, even this small value of efficiency is comparable to the sulfide removal capabilities of processes such as adsorption which concludes that neither of them is recommended for the same purpose.

5. Conclusion

The treatment of a spent-caustic effluent sample from the olefin unit of a petrochemical complex was studied in this work through the photocatalytic technique utilizing synthetic photocatalyst TiO_2-CTAB. The effective factors on the amount of COD removal were examined including the amount of oxidizing agent, aeration rate, pH and the amount of catalyst loaded. It was shown that all factors except pH have a positive effect on the removal efficiency. It was also concluded that aeration rate and utilized photocatalyst concentration are independent factors and have no simultaneous impact on the COD removal efficiency. Eventually, it was found that the presented technique has promising potential for removing phenol in the sample effluent, while it is inefficient in reducing the sulfide from the effluent solution.

References

[1] M. Bahri, A. Mahdavi, A. Mirzaei, A. Mansouri, F. Haghighat, Integrated oxidation process and biological treatment for highly concentrated petrochemical effluents: a review, Chem. Eng. Process. Process Intensif., 125 (2018) 183–196.
[2] I.B. Hariz, A. Halleb, N. Adhoum, L. Monser, Treatment of petroleum refinery sulfidic spent caustic wastes by electrocoagulation, Sep. Purif. Technol., 107 (2013) 150–157.
[3] A.I. Rita, C.S.D. Rodrigues, M. Santos, S. Sanches, L.M. Madeira, Comparison of different strategies to treat challenging refinery spent caustic effluents, Sep. Purif. Technol., 253 (2020) 117482, doi: 10.1016/j.seppur.2020.117482.
[4] C. Wu, Z. Gao, Y. Zhou, M. Liu, J. Song, Y. Yu, Treatment of secondary effluent from a petrochemical wastewater treatment plant by ozonation-biological aerated filter, J. Chem. Technol. Biotechnol., 90 (2015) 543–549.
[5] S. Shokrollahzadeh, F. Azizmohseni, F. Golmohammad, H. Shokouhi, F. Khademhaghighat, Biodegradation potential and bacterial diversity of a petrochemical wastewater treatment plant in Iran, Bioresour. Technol., 99 (2008) 6127–6133.
[6] M.Y. Ghaly, T.S. Jamil, I.E. El-Seesy, E.R. Souaya, R.A. Nasr, Treatment of highly polluted paper mill wastewater by solar photocatalytic oxidation with synthesized nano-TiO_2, Chem. Eng. J., 168 (2011) 446–454.
[7] G. Sivalingam, K. Nagaveni, M.S. Hegde, G. Madras, Photocatalytic degradation of various dyes by combustion synthesized nano anatase TiO_2, Appl. Catal., B, 45 (2003) 23–38.
[8] L. Zhong, F. Haghighat, Modeling and validation of a photocatalytic oxidation reactor for indoor environment applications, Chem. Eng. Sci., 66 (2011) 5945–5954.
[9] M. De Graaff, M.F. Bijmans, B. Abbas, G.-J. Euverink, G. Muyzer, A.J. Janssen, Biological treatment of refinery spent caustics under halo-alkaline conditions, Bioresour. Technol., 102 (2011) 7257–7264.
[10] T.M.S. Carlos, C.B. Maugans, Wet Air Oxidation of Refinery Spent Caustic: A Refinery Case Study, NPRA Conference, 2000, pp. 1–12.
[11] S.-H. Sheu, H.-S. Weng, Treatment of olefin plant spent caustic by combination of neutralization and Fenton reaction, Water Res., 35 (2001) 2017–2021.
[12] N. Rodriguez, H.K. Hansen, P. Nunez, J. Guzman, Spent caustic oxidation using electro-generated Fenton's reagent in a batch reactor, J. Environ. Sci. Health Part A, 43 (2008) 952–960.
[13] P. Nunez, H.K. Hansen, N. Rodriguez, J. Guzman, C. Gutierrez, Electrochemical generation of Fenton's reagent to treat spent caustic wastewater, Sep. Sci. Technol., 44 (2009) 2223–2233.
[14] Z. Yu, D. Sun, C. Li, P. Shi, X. Duan, G. Sun, J. Liu, UV-catalytic treatment of spent caustic from ethene plant with hydrogen peroxide and ozone oxidation, J. Environ. Sci., 16 (2004) 272–275.
[15] A. Hawari, H. Ramadan, I. Abu-Reesh, M. Ouederni, A comparative study of the treatment of ethylene plant spent caustic by neutralization and classical and advanced oxidation, J. Environ. Manage., 151 (2015) 105–112.
[16] S.H.Y. Sayid Abdulah, M.A. Abu Hassan, Z.Z. Noor, A. Aris, Optimization of Photo-Fenton Oxidation of Sulfidic Spent Caustic by Using Response Surface Methodology, 2011 National Postgraduate Conference (NPC), IEEE, Perak, Malaysia, 2011, pp. 1–7.

[17] C. Chen, Wet air oxidation and catalytic wet air oxidation for refinery spent caustics degradation, J. Chem. Soc. Pak., 35 (2013) 244–250.
[18] M. Alaiezadeh, Spent Caustic Wastewater Treatment with Electrical Coagulation Method, The 1st International Conference Oil, Gas, Petrochemical and Power Plant, Tehran, Iran, 2015.
[19] A.A. Ansari, M. Kamil, Kabir-ud-Din, Polymer-surfactant interactions and the effect of tail size variation on micellization process of cationic ATAB surfactants in aqueous medium, J. Dispersion Sci. Technol., 34 (2013) 722–730.
[20] J. Medina-Valtierra, M. Sánchez-Cárdenas, C. Frausto-Reyes, S. Calixto, Formation of smooth and rough TiO_2 thin films on fiberglass by sol-gel method, J. Mexican Chem. Soc., 50 (2006) 8–13.
[21] G.Q. Liu, Z.G. Jin, X.X. Liu, T. Wang, Z.F. Liu, Anatase TiO_2 porous thin films prepared by sol-gel method using CTAB surfactant, J. Sol-Gel Sci. Technol., 41 (2007) 49–55.
[22] H. Bazrafshan, Investigation and Synthesis of Catalytic Nanoparticles Suitable for Decomposition of Water by Sunlight to Produce Hydrogen, Amirkabir University of Technology, Tehran, Iran, 2013.
[23] W.E. Federation, A.P.H. Association, Standard Methods for the Examination of Water and Wastewater, American Public Health Association (APHA), Washington, DC, USA, 2005.
[24] U.I. Gaya, A.H. Abdullah, Heterogeneous photocatalytic degradation of organic contaminants over titanium dioxide: a review of fundamentals, progress and problems, J. Photochem. Photobiol., C, 9 (2008) 1–12.